Multiscale model of the PECM with oscillating cathode for external geometries using a virtual switch

I. Schaarschmidt[1],G. Meichsner[2], M. Zinecker[1], M. Hackert-Oschätzchen[1], A. Schubert[1,2]
[1]Professorship Micromanufacturing Technology, Chemnitz University of Technology, 09107 Chemnitz, Germany
[2]Fraunhofer Institute for Machine Tools and Forming Technology, 09126 Chemnitz, Germany

Introduction

The pulsed electrochemical machining (PECM) with oscillating cathode is a further development of the conventional electrochemical machining (ECM). ECM is based on the principle of the material dissolution due an electrochemical reaction at the interface between the anode and an ion conductor, the electrolyte. The anode, which is the workpiece, is connected to a positive electric potential, while the cathode, which is the tool, is connected to the ground with an electric potential of zero. The area between the anode and the cathode is referred to as the working gap and is filed with the electrolyte. [1], [2]
ECM is a contact free process and in consequence, the workpiece is not influenced due heating or mechanical stress. Another characteristic of ECM is that the material dissolution is independent from the mechanical properties of the workpiece. [3]
During the material dissolution hydrogen and heat formation take place within the working gap. Both processes, together with occurrence of dissolution products, influences the electric conductivity of the electrolyte. This leads to a change of the process conditions. Undesirable consequences are deviation of the shape or abort of the ECM-process. [3]
To avoid those consequences and achieve geometries that are more precise, flushing of the working gap with fresh electrolyte is necessary.
To optimize the flushing process**,** the pulsed electrochemical machining (PECM) with oscillating cathode was developed. Figure 1 shows the principle and phases of the pulsed electrochemical machining with oscillating cathode. In the first step, the cathode and anode are aligned to each other and the electrolyte flow is started. In the second step the cathode moves along the z-axis direction towards the anode (workpiece) and a short current pulse is initiated at the bottom dead center of the cathode oscillation. At this point, the material dissolution begins and reaction products like hydrogen, dissolved material and process heat influence the electric conductivity of the electrolyte inside the working gap. After this, the electric current is paused and the cathode moves back to the top dead center of the cathode oscillation in the third step. The working gap increases and is flushed with sufficiently conductive electrolyte before a new electric pulse is triggered again at the new bottom dead center of the oscillation [4].

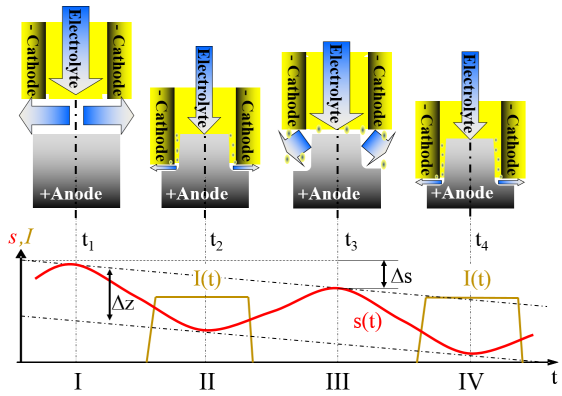

Figure 1: Principle of the pulsed electrochemical machining (PECM) with oscillating cathode (*s* - Movement of cathode, *I* - electric current)

A good example for an application of PECM is manufacturing of impact extrusion punches. The requirements for the punches in mass production are good wear resistance and very high precision. To reduce the wear and increase the lifetime, wear resistant materials like powder metallurgy steels (PM-steels) are needed. These materials are characterized by high hardness and high ductility [4]. PECM allows the machining of hardened or powder metallurgical steels without any wear of the tool (cathode) in combination with a very high precision.
However, in practice, the designing of the machining parameters and tool design are very time-consuming and cost intensive empirical procedures.
Multiphysics simulation supports the process and tool design. The main challenge performing simulations of PECM with oscillating cathode is the implementation of different physical phenomena that occur in strongly different time scales.
This study presents an implementation technique of a multiscale multiphysics approach for PECM with oscillating cathode using COMSOL Multiphysics as a further development of previous work shown in [5]. This study addresses the implementation of the simulation steps of different time scales within one comprehensive model by modeling a virtual switch.

This virtual switch allows switching between the short and the long time scale phenomena without stopping the simulation and realizes the correlation of the single physical phenomena and boundary condition to the respective time scale.

Geometry and Material Parameters

The design concept of electrochemical machining of external geometries such as extrusion punches, is shown in Figure 2. Significant elements of the design concept are the workpiece (gray), the cathode (yellow) and the insulation (green). The cathode has an inner diameter of 16.4 mm with a thickness of 5 mm. The inner side of the cathode has a chamfer with an angle of 45° and length of 4 mm. The workpiece has an outer diameter of 20 mm at the beginning of the processing.

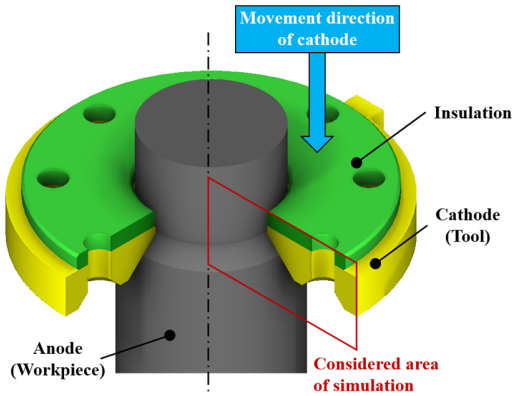

Figure 2: Design concept for machining of external geometries and position of the considered area of simulation

The movement direction of the cathode is along the z-axis. The whole concept is nearly axisymmetric. Figure 3 represents the initial model geometry derived from the design concept containing the numbering of domains and boundaries.

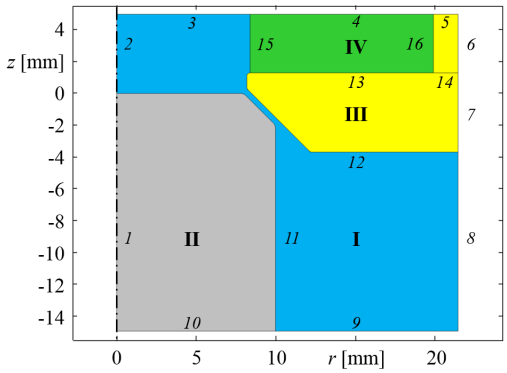

Figure 3: Derived initial 2D-axisymmetric geometry (t = 0 s) of the concept containing the numbering of domains and boundaries

Domain I (blue) is the electrolyte. In this study, an electrolyte with a mass fraction of 8% sodium nitrate ($NaNO_3$) is considered and defined as a fluid. The anode, or workpiece, is represented in domain II (grey). The workpiece material is a powder metallurgical steel, named CPM REX T15 and is defined as solid. The cathode, which is also the tool, is defined in domain III (yellow) as solid and is made from a copper alloy named MS58). The green domain IV is the insulation and is made from Polyoxymethylen (POM). The implemented material parameters are summarized in Table 1. Here ρ is the density, σ the electric conductivity, λ the thermal conductivity and c_p the heat capacity.

Table 1: Material parameters of the simulation model

Domain	Materials	ρ [kg/m³]	σ [S/m]	λ [W/(m·K)]	c_P [J/(kg·K)]
I	Electrolyte	1025.5	$\sigma_{eff}(\phi_{El},T)$	0.599	3877
II	REX T15	8190	$1 \cdot 10^6$	24,2	4700
III	MS58	8470	$15 \cdot 10^6$	123	3770
IV	POM	1410	10^{-10}	0.31	1500

The effective electric conductivity of the electrolyte σ_{eff} depends on the volume fraction of the generated hydrogen bubbles and the temperature. Equation (1) describes the effective electric conductivity of the electrolyte as a function of temperature T and hydrogen volume fraction ϕ_{H_2}. An increase of hydrogen concentration lead to a decrease of the effective electric conductivity of the electrolyte [6].

$$\sigma_{eff}(T,\phi_{El}) = \sigma_{El}(T) \cdot (1-\phi_{H_2})^{\frac{3}{2}} \quad (1)$$

Further $\sigma_{El}(T)$ represents the experimentally determined conductivity of the pure electrolyte with a mass fraction of 8% $NaNO_3$ as a function of the temperature and is described by equation (2).

$$\sigma_{El}(T) = 1.646\,\frac{mS}{cm}\left(\frac{T}{1\mathrm{K}} - 273.15\right) + 39.796\,\frac{mS}{cm} \quad (2)$$

The remaining material parameters are assumed to be constant.

Physics and boundary conditions

The multiscale simulation model is divided in two simulation steps, simulation step A and simulation step B. A detailed explanation of the multiscale approach is shown in [5].
Figure 4 represents the scheme of the simulation model. It is obvious that each simulation step

considers different physical phenomena. Simulation step A includes the physical phenomena of the short time scales such as the electro-, thermo- and fluid dynamics as well as the oscillation of the cathode. Simulation step B considers the physical phenomena of long time scales such as the constant movement of the cathode and the material dissolution.

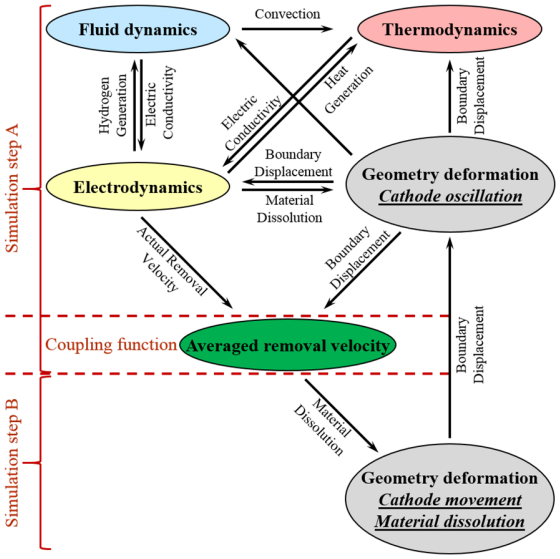

Figure 4: Principle and considered physical phenomena of the simulation model and correlation to the simulation steps

The simulation was performed with a fully coupled model. The interfaces of electric currents, heat transfer in fluids and deformed geometry for modeling the material dissolution and the cathode movement were used. Fluid dynamics, including the formation and transport of hydrogen together with the electrolyte, is modeled by a potential two-phase flow in domain I. The inlet of the electrolyte flow is set on boundary 9 and the outlet on boundary 3. The generation of hydrogen only occurs on boundary 12, the cathode surface. For further information of modeling and implementation of the fluid dynamics, refer to reference [7]. The thermodynamics interface is solved for every domain. Joule heating is considered on the electrode-electrolyte interfaces (boundaries 11 and 12) and is a result of the energy conversion due the electric over potential in the electrochemical double layer. The over potentials according to experimental results with 5 V at the anode-electrolyte and 1 V at the cathode-electrolyte interface.

The electrodynamics interface is solved in every domain. Electric insulation is set on boundary 2-4 and 6-9. The ground potential ($U = 0$ V) is set on boundary 5. The process Voltage $\hat{\varphi}$ is set on boundary 10 and defined as a rectangle function with a maximum of 8 V and a pulse-on time t_{on} of 4 ms with a cycle duration c of 0.02 s.

The movement of the cathode s_z is defined as a superimposition of the constant movement and the oscillation of the cathode in z-direction and is described by equation (3) using the deformed geometry interface. Here $\hat{s}$ is the amplitude and f the frequency of the oscillation. The variable $\hat{X}$ is the discrete state variable, which defines the correlation to the discrete simulation step. $\hat{X}$ is described in more detail later. The parameter v_z is the constant movement speed of the cathode.

$$s_z = \underbrace{\left(\hat{s} \cdot cos\left(2\pi \cdot f \cdot t + \frac{\pi}{2}\right)\right) \cdot \hat{X}}_{\text{Oscillation of cathode}} - \underbrace{v_z \cdot t}_{\substack{\text{constant} \\ \text{Movement}}} \qquad (3)$$

Equation (3) is defined at boundary 12-14. The electric current leads to electrochemical reaction at the anode surface and in consequence to the removal of the workpiece surface. To consider this phenomenon, the material-specific removal speed $\vec{v}_a$, which is a function of the normal current density, is defined at the anode surface (boundary 11).

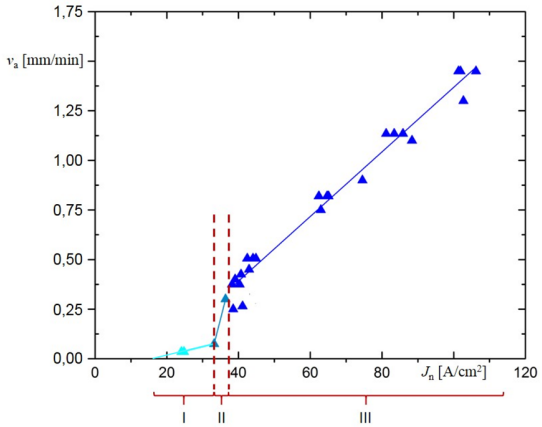

Figure 5: Material specific removal velocity $\vec{v}_a$ as function of the normal current density J_n

$\vec{v}_a$ is a result of experimental investigations to determine the removal characteristics of the workpiece material and is shown in Figure 5 [8]. The function is implemented as a piecewise function consisting of four single linear functions. It is obvious that the material dissolution ($\vec{v}_a > 0$ mm/min) starts at 17 A/cm^2. Table 2 summarizes the constant input parameters.

Table 2: Summary of the constant input parameters of the simulation

Symbol	Definition	Value	Unit
c	Cycle duration	0.02	s
f	Frequency of oscillation	50	Hz
p_{Out}	Outlet absolute pressure	7	bar
$\hat{\varphi}$	Electric Potential	8	V
$\hat{s}$	Amplitude of oscillation	200	µm
t_{on}	Pulse on time	4	ms
$\dot{V}_{El}$	Electrolyte flow rate	6	l/min
v_z	Constant movement velocity	0.1	mm/min
T_U	Ambient Temperature	20	°C

The coupling function between the simulation step A and the simulation step B is the averaged removal velocity and is a User-Defined-Equation (UDE) at the anode surface (boundary 11). Equation 4 shows the mathematical description of the coupling function. The variable s_a is the distance of the movement of the anode surface due to the material removal.

$$\bar{v}_a = \frac{1}{t_a} \cdot s_a = \frac{1}{t_a} \cdot \int_t^{t+t_a} v_{a,i}(J_n)\, dt \qquad (4)$$

Input variable is the actual removal velocity, which is a function of the normal current density and is shown in Figure 5.

Virtual switch modelling

For modelling the virtual switch, it is necessary to define the change from simulation step A to simulation step B and back from simulation step B to simulation step A. This is achieved by using the Events interface. It is required to define four variables to describe the virtual switch. The discrete state variable $\hat{X}$ is used to be the discrete variable which separates both simulation steps and the related physical phenomena and boundary conditions. Furthermore, two indicator state variables are defined. One is the start indicator variable I_{start} which defines the begin of the simulation step A within the short time scale physical phenomena are considered. The other is the stop indicator variable I_{stop}, which defines the end of the simulation step A, and the start of the simulation step B. The simulation step B considers the long time scale physical phenomena. To control the time range for every simulation step, the global time variable t_G is defined. Below every variable is described in detail.

Discrete state variable

The discrete state variable $\hat{X}$ is the variable, which represents the switch-variable connecting to the physical equations and boundary conditions. This variable can be either zero or one. If $\hat{X}$ is equal one, simulation step A is active and the physical phenomena of the short time scales, like pulsed electric current, heat and hydrogen generation and cathode oscillation are considered. If $\hat{X}$ is equal zero, simulation step B is active and the physical phenomena of long time scales, like movement of the cathode and material dissolution are calculated.
Through modifying the governing equations by multiplying them with the switch-variable $\hat{X}$, it is possible to match them to the concrete time step and in consequence to the time scale group. The switch-variable $\hat{X}$ can be changed by reinitialize it when an implicit event, like the start or end of a simulation step occurs. The initial condition is zero that means the simulation starts with simulation step B, which considered the physical phenomena of the long time scales and the first event appears after a defined time of 2 s.

Global time variable

The global time variable t_G is defined as a global ordinary differential equation. The reason for an additional equation, which counts the time, is the possibility to reinitialize this variable if it is necessary, for example when an implicit event occurs.

$$t_G = t \qquad (5)$$

Start indicator variable

The start indicator variable I_{start} defines the begin of the simulation step A within the physical phenomena of the short time scales are calculated and the simulation step B ends.

$$I_{start} = t_G - t_B = t_G - \frac{s_f}{v_z} \qquad (6)$$

This event occurs whenever I_{start} is equal to zero. Equation (6) represents the definition of I_{start}. Here s_f is the movement distance of the cathode and is implemented as a constant input parameter in this simulation model.
Another functionality is the reinitialization of different variables immediately when the start indicator variable is zero and this event occurs. The discrete state variable $\hat{X}$ is set to one; the global time variable and the distance of the movement of the anode surface due to the material removal s_a are set to zero.

Stop indicator variable

The stop indicator variable I_{stop} defines the end of the simulation step A and the start of the simulation step B and is described by equation (7).

$$I_{\text{stop}} = t_{\text{G}} - t_{\text{A}} = t_{\text{G}} - i \cdot \frac{1}{f} \qquad (7)$$

Here f is the frequency of the cathode oscillation and i the number of how many cycle duration of the cathode oscillation are considered.

As soon as the indicator variable I_{stop} is equal to zero this event occurs and the discrete state variable $\hat{X}$ is reinitialized and is set to zero.

An overview of all variables, which are reinitialized when an event occurs, is shown in table 3.

Table 3: Reinitialized variables and correlation to the event

Event	Variables	Value
$I_{\text{start}} = 0$: Start of step A; End of step B	t_{G}	0
	$\hat{X}$	1
	s_a	0
$I_{\text{stop}} = 0$: End of step A; Start of step B	$\hat{X}$	0

Meshing

The mesh of the simulation model is shown in Figure 6. The left side in Figure 6 represents the overview of the mesh of the whole geometry. The right picture in Figure 6 represents a detailed view of the mesh of the working gap.

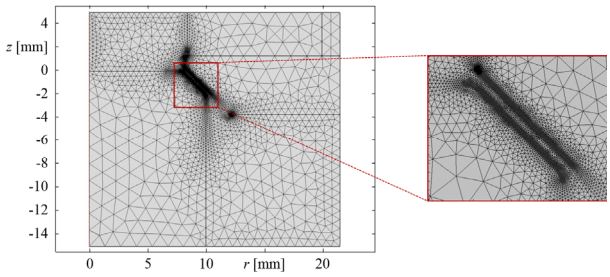

Figure 6: Initial mesh for the simulation; left: overview; right: detail of the working gap

It is obvious that the mesh is refined in the area of the working gap where the most significant changes of the field variables are expected. Furthermore, in a later stage of the simulation a massive change of the geometry due to the movement and oscillation of the cathode, also to the material dissolution is expected. This leads to a distortion of the mesh and in consequence to a change in the mesh quality. To avoid too low mesh quality, the automatic remeshing feature is used with a solver stop and remeshing condition when the distortion exceeds 0.5.

Summarizing the initial mesh consists of 10054 triangle-elements. The minimal element size is 3 µm and a maximal size is 1.44 mm. To realize a mesh refinement in the area of the working gap a resolution factor for narrow regions is set to 15.

Results

In Figure 7 the virtual switch modeling is shown. It can be seen that the virtual switch variables change with time. For a better representation, the variables are scaled. The global time variable (black), the start indicator (grey) and stop indicator (blue) increase with time until the start event occurs, when the start indicator reaches a value of zero. The reinitialization of all virtual switch variables can be seen here. The discrete state variable, which is connected to the physical phenomena equations, changes from zero to one.

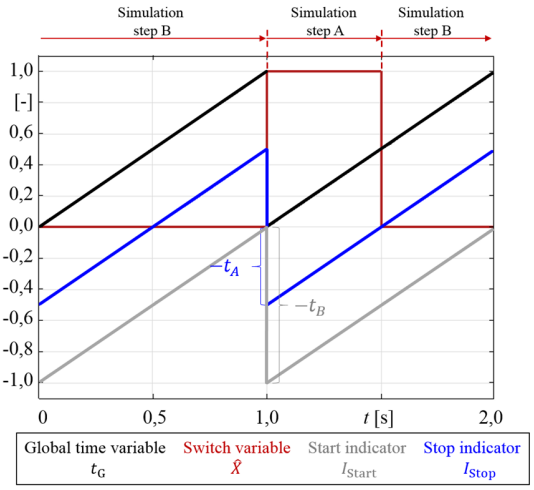

Figure 7: Switch variables as function of time (schematic)

Now the simulation step A starts within the physical phenomena of short time scales are simulated.

To illustrate the principle of the virtual switch modeling in more detail, the movement of the cathode can be seen in Figure 8. The movement of the cathode is defined by equation (3) and combines the superimposed motion of the cathode with the virtual switch modeling.

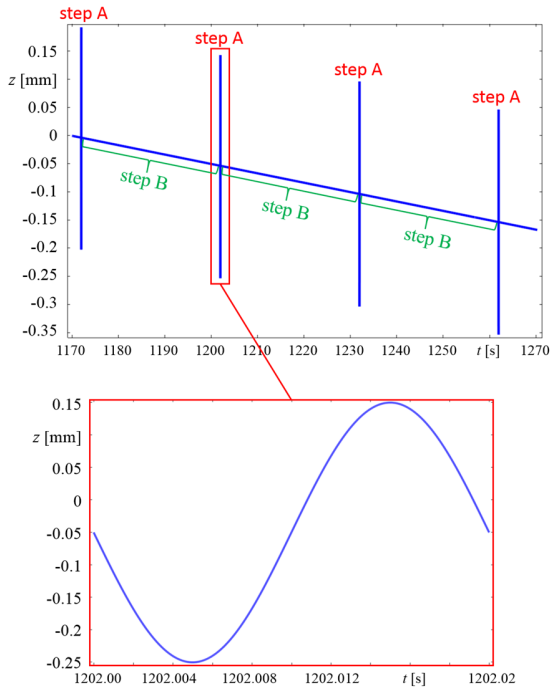

Figure 8: Movement of the cathode regarding multiple iterations of simulation step A and simulation step B (upper figure); Detailed representation within simulation step A (lower figure)

It is obvious that the movement of the cathode is not a continuous oscillating motion in the present simulation model. The simulation step A occurs every 30 s. In this 30 s, the cathode moves over a distance of 50 µm with a movement velocity of 0.1 mm/min. At the same time different physical phenomena and processes of simulation step A occur. To regard and analyze all those physical phenomena are not the focus of this work. Furthermore it is obvious, that only every 1500th cathode oscillation is simulated. This results in a very low computational effort.

The most relevant variable to simulate the material dissolution of the workpiece is the resulting actual material specific removal velocity at the anode (workpiece) surface.

Figure 9 shows the removal velocity $\vec{v}_a$ distribution along the anode surface while the cathode is at the bottom dead center of the oscillation at the process time of 1202.005 s (Step A). It can be seen that the maximum of the actual removal velocity occurs in the area of the angular face of the anode. The removal velocity $\vec{v}_a$ decreases along the vertical anode surface. The rapid drop of the removal velocity (at $z = -1.7$ mm) is a consequence of implementing of the material specific removal velocity of the anode material REX T15.

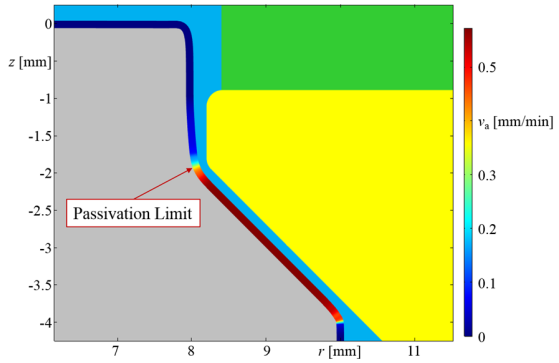

Figure 9: Actual removal velocity $\vec{v}_a$ distribution along the anode surface at a process time of 1202.005 s

The rapid drop from 0.5 mm/min to 0.1 mm/min marked the passivation limit of the considered material.

Figure 10 shows the correlation of the maximum actual and maximum averaged material removal velocity as a function of the time. The actual removal velocity is approximately 7 times bigger then the averaged removal velocity.

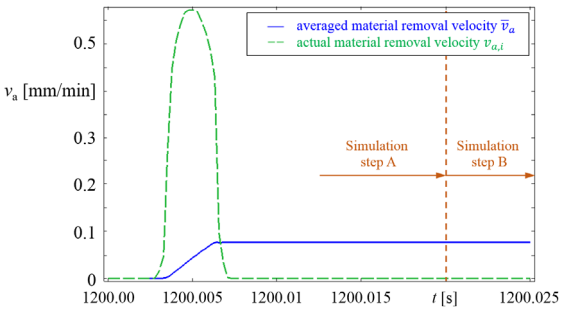

Figure 10: Correlation between the actual removal velocity and the averaged material removal velocity as a function of the process time [5]

With this evaluated value the material dissolution in simulation step B is simulated for 30 s until the start indicator variable reaches a value of 0 and the simulation step A starts again.

Figure 11 illustrates the resulting material dissolution after a long process time of 1600 s with using the multiscale approach in combination with the virtual switch. The motion of the cathode and insulation is neglected due to a clearer representation.

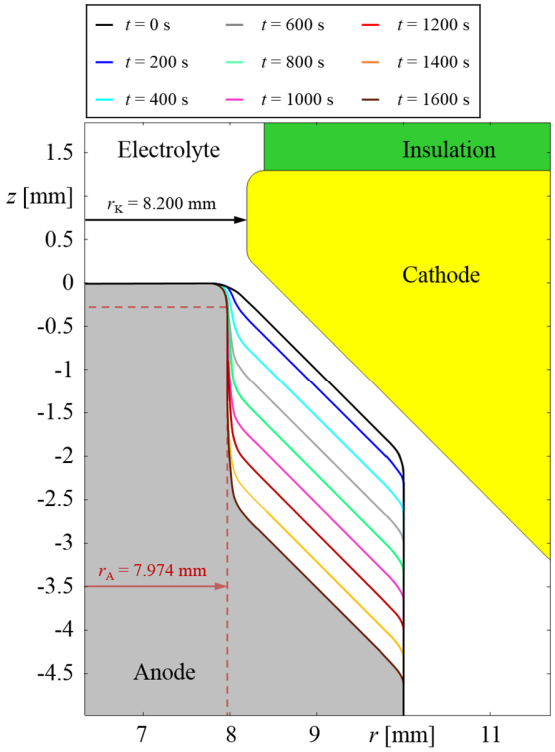

Figure 11: Detailed view of the forming process due the material dissolution after a process time of 1600 s

It can be seen that the resulting radius of the workpiece is 7.974 mm, which leads to a side working gap of 226 µm.

Conclusions

In this study, the implementation of a multiscale approach of the PECM with oscillating cathode using a virtual switch was shown. The whole simulation model consists of two study steps. Simulation step A considers the physical phenomena of the short time scales and the simulation step B the physical phenomena of the long time scales. Both simulation steps are coupled by a coupling function of the updated geometry. The advantage of using this switch is reducing of computational effort and the avoidance of import and export of changed geometries and variables.
In future work the start indicator variable should be implemented as an inconstant value. Instead, the constant parameter of s_z and v_f, the start indicator variable can depends of the change rate of the anode surface. This leads to a self-controlled simulation model and can reduce the computational effort further. Furthermore the experimental investigation of the PECM with oscillating cathode for machining external geometries and the comparison with achieved simulation results

References

[1] F. Klocke and W. König, *Fertigungsverfahren 3; Abtragen, Generieren und Lasermaterialbearbeitung*. Berlin: Springer-Verlag, 2007, ISBN: 978-3-540-48954-2
[2] M. Hackert-Oschätzchen, "Gestaltung von elektrochemischen Abtragprozessen durch Multiphysiksimulation gezeigt an der Endformgebung von Mikrobohrungen (Habilitationsschrift)," in *Schubert, A. (Hrsg.): Scripts Precision and Microproduction Engineering, Band 10*, Verlag Wissenschaftliche Scripten, 2015
[3] A. E. DeBarr and D. A. Oliver, *Electrochemical Machining*. New York: American Elsevier Pub. Co., 1968
[4] W. Schatt and K. W. B. Kieback, *Pulvermetallurgie- Technologien und Werkstoffe*. ISBN: 9783540236528
[5] I. Schaarschmidt et al., "Multiscale Multiphysics Simulation of a Pulsed Electrochemical Machining Process with Oscillating Cathode for Microstructuring of Impact Extrusion Punches," *Procedia CIRP*, vol. 58, pp. 257–262, 2017, ISSN: 22128271
[6] J. A. McGeough, *Principles of electrochemical machining*. London: Chapman and Hall, 1974
[7] M. Hackert-Oschätzchen et al., "2-D Axisymmetric Simulation of the Electrochemical Machining of Internal Precision Geometries," in *Proceeding of the European COMSOL Conference*, 2016, p. 7
[8] G. Meichsner et al., "Fast Determination of the Material Removal Characteristics in Pulsed Electrochemical Machining," in *CIRP Conference on High Performance Cutting - HPC 2016*, 2016, vol. 46, pp. 123–126, ISSN: 22128271

Acknowledgements

This project is funded by the Federal Ministry of Economics and Technology, following a decision of the German Bundestag.